

UDK: 535.375; 535.37

## Characterization of Neodymium Doped Calcium Tungstate Single Crystal by Raman, IR and Luminescence Spectroscopy

Rouaida Mohamed Abozaid<sup>1</sup>, Zorica Ž. Lazarević<sup>2\*</sup>), Vesna Radojević<sup>1</sup>, Maja S. Rabasović<sup>2</sup>, Dragutin Šević<sup>2</sup>, Mihailo D. Rabasović<sup>2</sup>, Nebojša Ž. Romčević<sup>2</sup>

<sup>1</sup>Faculty of Technology and Metallurgy, University of Belgrade, Belgrade, Serbia

<sup>2</sup>Institute of Physics, University of Belgrade, Pregrevica 118, Zemun, Belgrade, Serbia

### Abstract:

The aim of the current work was to assess obtain a single crystal of calcium tungstate doped with neodymium - ( $\text{CaWO}_4:\text{Nd}^{3+}$ ), and after that, the crystal was characterized with various spectroscopic methods. The single crystal was grown from the melt using the Czochralski method in air. By optimizing growth conditions,  $\langle 001 \rangle$ -oriented  $\text{CaWO}_4:\text{Nd}^{3+}$  crystals up to 10 mm in diameter were grown. Number of dislocations in obtained crystal was  $10^2$  per  $\text{cm}^2$ . Micro hardness was measured with the Vickers pyramid. Anisotropy in  $\langle 001 \rangle$  direction was not observed. Selected  $\text{CaWO}_4:\text{Nd}^{3+}$  single crystal was cut into several tiles with the diamond saw. The plates were polished with a diamond paste. The crystal structure is confirmed by X-ray diffraction. The obtained crystal was studied by Raman and infrared spectroscopy. Seven Raman and six IR optical active modes predicted by group theory are observed. FTIR confirmed the occurrence of all the functional groups and bonds in this material. From the FTIR spectrum, a strong peak of  $862 \text{ cm}^{-1}$  has been obtained due to the stretching vibration of  $\text{WO}_4^{2-}$  in scheelite structure, and a weak but sharp band at  $433 \text{ cm}^{-1}$  has been noticed due to the metal-oxygen (Ca-O) band. Estimated luminescence lifetime of  $^4F_{5/2}$  - the  $^4I_{9/2}$  transition is about  $120 \mu\text{s}$ ; estimated luminescence lifetime of  $^4F_{3/2}$  - the  $^4I_{9/2}$  transition is about  $140 \mu\text{s}$ . All performed investigations show that the obtained  $\text{CaWO}_4:\text{Nd}^{3+}$  single crystal has good optical quality, which was the goal of this work.

**Keywords:**  $\text{CaWO}_4:\text{Nd}^{3+}$ ; Raman spectroscopy; IR spectroscopy; Luminescence.

## 1. Introduction

In recent years, molybdates and tungstates belonging to the scheelite-type tetragonal structure [1-4] have been extensively investigated by the scientific community for technological applications in acousto-optic filters [5], solid state lasers [6, 7], light-emitting diodes [8], photocatalysts [9, 10], phosphors [11-13], scintillators [14-16], microwave dielectrics [17, 18], and cryogenic scintillation detectors [19, 20]. Among these materials, the pure or rare earth-doped calcium tungstate ( $\text{CaWO}_4$ ) has been studied because of its photoluminescence (PL) emissions in the visible wavelength regions of the electromagnetic spectrum [21-25].

Tungsten and its alloys because of their unique characteristic have wide application in many sectors of the industrial production [26]. Calcium tungstates are natural minerals.

<sup>\*</sup> Corresponding author: [lzorica@yahoo.com](mailto:lzorica@yahoo.com)

Furthermore, they can be made synthetically. The mineral name associated with these materials is  $\text{CaWO}_4$ . The name used to describe the common crystal structure of these materials is scheelite [27]. The scheelite- $\text{ABO}_4$  ( $A=\text{Ca}$  and  $B=\text{W}$ ) crystal structure (Figure 1) is characterized by the tetragonal space group  $I4_1/a$  ( $n^\circ 88$ ). The B atoms are surrounded by four O atoms in an approximately tetrahedral symmetry configuration, and the A atoms are surrounded by eight O atoms in an approximately octahedral symmetry. Many material properties can be associated to the existence of these  $[\text{BO}_4]$  (Fig. 1b) and  $[\text{AO}_8]$  (Fig. 1a) approximate polyhedrons into crystalline structure. The B cation tetrahedra (with W) behave as rigid structural elements with no observed cation oxygen compression [28]. On the other hand, compression of the eight-coordinated  $A=\text{Ca}$  polyhedron, is more favorable parallel to  $c$  than perpendicular to  $c$  [26].

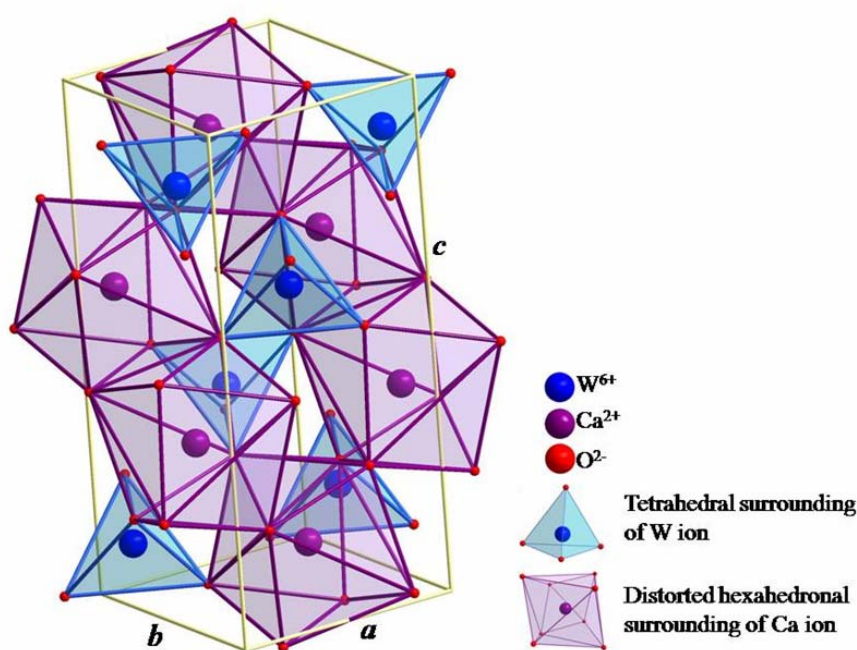


**Fig. 1.** Unit cell of  $\text{CaWO}_4:\text{Nd}^{3+}$  single crystal.

Various techniques such as the Czochralski technique, flux method, and solid-state reactions have been used to synthesize single crystals, whiskers, and powder of  $\text{CaWO}_4:\text{Nd}^{3+}$  [29]. Some attempts were made on the preparation of single crystal films, but these experiments had limited success because of the high vaporization pressure of  $\text{WO}_3$  and obtained films did not have a uniform structure. The growth of single crystals from melt by the Czochralski method has a number of advantages, such as the absence of contact between the crystal and the crucible walls, that essentially reduces stresses in the crystals; the possibility to control the crystal growth visually and the processes which occur at crystal-melt interface, relative simplicity of its technical realization. Moreover, the method allows to grow large-size and sufficiently perfect high-melting oxide crystals, to control the character of the melt convection and as consequence to choose the most optimal conditions for the growth of optically homogeneous crystals. Possibilities of the method are able to provide the obtaining of crystals of different shape.

The aim of our work was to produce neodymium doped calcium tungstate single crystal ( $\text{CaWO}_4:\text{Nd}^{3+}$ ) good optical quality. The  $\text{Nd}^{3+}$  content was 0.8 at. %, as is usual for laser materials. The structural and optical properties obtained crystal was characterized using Raman, IR and luminescence spectroscopy.

## 2. Materials and Experimental Procedures

Czochralski method was used to obtain single crystals of  $\text{CaWO}_4:\text{Nd}^{3+}$ . The observations relating to the dislocation were recorded by observing an etched surface of  $\text{CaWO}_4:\text{Nd}^{3+}$  crystal, using a Metaval of Carl Zeiss Java metallographic microscope with magnification of 270x. A selected  $\text{CaWO}_4:\text{Nd}^{3+}$  single crystal was cut into several tiles with the diamond saw. The plates were polished with a diamond paste, which were later used for the characterization of Raman, IR and luminescence spectroscopy. The crystal plane of cleavage of  $\text{CaWO}_4:\text{Nd}^{3+}$  crystal is  $\langle 001 \rangle$ . Thin panels for testing dislocations we obtained by splitting of individual pieces of crystal. A solution for etching the crystals consisted of one part of 40 % HF and the two parts of a saturated solution of  $\text{CrO}_3$ . The sample was etched for 15 min.

Hardness of samples was obtained by Vickers microhardness tester “Leitz, Kleinhartepuffer DURIMET I”, using the load of 4.9 N. Three indentations were made at each load, yielding six indentation diagonals measurements, from which the average hardness could be calculated. The indentation was done at room temperature.

The structural characteristics were obtained by the XRD powder technique using Philips PW 1050 diffractometer equipped with a PW 1050 generator, 40kV x 20mA, using Ni filtered  $\text{Co K}\alpha$  radiation of  $\lambda = 1.54178 \text{ \AA}$  at room temperature. Measurements were carried out in the range of  $10\text{-}90^\circ$  with a scanning step of  $0.05^\circ$  and scanning time 4 s per step. Unit cell parameters were determined by Le Bail’s full profile refinement using *FullProf* computing program. The crystallite size and microstrain were determined by using X-Fit software packages which is based on Fundamental Parameter convolution approach [30].

Raman spectra measurements were performed on a system of Princeton TriVista 557 triple monochromator and CCD detector (charged-coupled-device). As an excitation laser line is used the wavelength of 532 nm. Monochromator used the configuration 900/900/1800 point per millimeter, and a resolution of 1.5 inverse centimeters. The laser power at the sample amounted to 0.25 mW, a laser beam is focused on the sample by means of microscopic lenses with a magnification 50x. Spectra were recorded in the range from 100 to  $1200 \text{ cm}^{-1}$ .

The infrared reflectivity measurements were performed at room temperature with a BOMEM DA-8 Fourier-transform infrared spectrometer [31]. A hyper beamsplitter and deuterated triglycine sulfate (DTGS) pyroelectric detector were used to cover the wavenumber region from 80 to  $650 \text{ cm}^{-1}$ . Spectra were collected with  $2 \text{ cm}^{-1}$  resolution and with 500 interferometer scans added for each spectrum.

FTIR spectra of the samples in KBr discs were obtained by transmission spectroscopy (Hartmann & Braun, MB-series). The FTIR spectra were recorded between 4000 and  $400 \text{ cm}^{-1}$  wavenumber region at a resolution of  $4 \text{ cm}^{-1}$ .

The photoluminescence (PL) response is not simple [32]. Photoluminescence emission spectra can be used for investigation of the possible outcomes of photoinduced electrons and holes in a materials, since photoluminescence emission results from the recombination of free charge carriers [33]. The time resolved optical characteristics of samples were analyzed using streak camera and Nd:YAG laser as excitation source (Fig. 2). The setup is described in more detail in our earlier publication [34]. Shorty, the basic setup of time resolved laser induced fluorescence measurement system consists of Vibrant OPO laser system and Hamamatsu streak camera. The output of the OPO can be continuously tuned over a spectral range from 320 nm to 475 nm. The samples can be also excited by the second harmonic (532 nm) of the Nd-YAG OPO pump laser. After analysis of preliminary results, we decided to use excitation at 532 nm for time resolved analysis of  $\text{CaWO}_4:\text{Nd}^{3+}$  near infrared luminescence. This pulsed laser excitation has duration of about 5 ns and repetition rate 10 of Hz. The emission spectra were recorded using a streak scope (Hamamatsu model C4334-01) with integrated video streak camera.

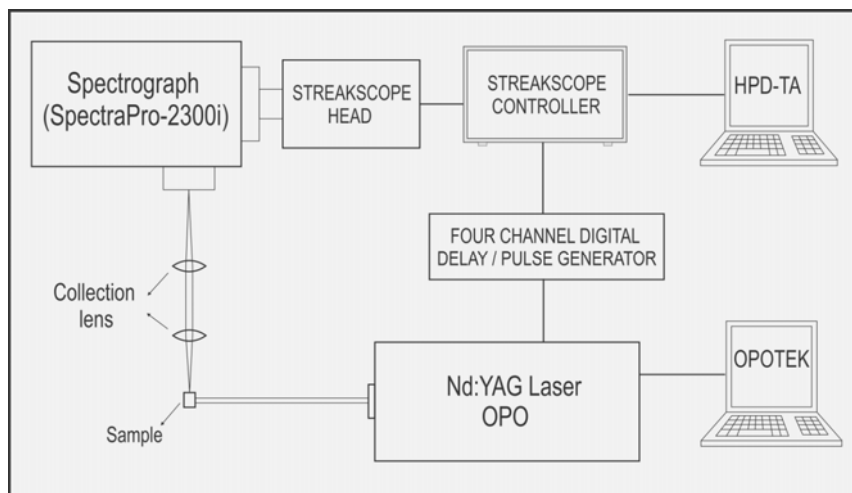


**Fig. 2.** Schematic illustration of experimental setup for time-resolved laser fluorescence (TRLIF).

### 3. Results and Discussion

$\text{CaWO}_4:\text{Nd}^{3+}$  single crystals were grown by the Czochralski technique in air. The best results were obtained with a crystal growth rate of  $6.7 \text{ mm h}^{-1}$ . The critical rotation rate was 30 rpm. The obtained single crystal was about 70 mm in length and 10 mm in diameter (Fig. 3).



**Fig. 3.** Photographs of  $\text{CaWO}_4:\text{Nd}^{3+}$  single crystal.

From the Fig. 4a), the dislocations can be observed. Number of dislocations in  $\text{CaWO}_4:\text{Nd}^{3+}$  crystal was 638 per  $\text{cm}^2$ . Before individual dislocations can be observed little corner of the border. One of them is shown in Fig. 4b).

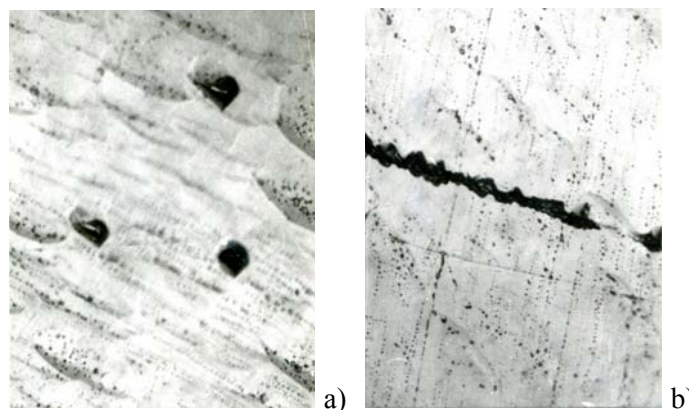


**Fig. 4.** The microscopic image of the surface  $\text{CaWO}_4:\text{Nd}^{3+}$  crystal plate in the direction  $\langle 001 \rangle$  after etching 15 min: a) appearance of individual dislocations and b) look of low-angle boundaries on the surface. Magnification of 270x.

Hardness of the samples was  $\text{HV} = 1.5 \text{ GPa}$ .

Structure of synthesized  $\text{CaWO}_4:\text{Nd}^{3+}$  powdered sample was identified by XRD pattern as shown in Fig. 5. The diffractogram confirms that sample is monophased, and that it crystallized in scheelite type of structure in 88. space group,  $I4_1/a$ . All of the observed diffraction peaks are indexed according to this space group. In this structural type, Ca ions occupy  $4b$  Wyckoff positions  $[[0, 1/4, 5/8]]$  with local symmetry  $\bar{4}$ , while W ions occupy  $4a$  Wyckoff positions  $[[0, 1/4, 1/8]]$  with the same local symmetry. W ions are in tetrahedral surrounding of O ions (coordination number 4), while Ca ions are in distorted hexahedral surrounding of O ions (coordination number 8) as shown in Fig. 1. W tetrahedrons share common vertices with Ca polyhedrons, while Ca polyhedrons between each other share common edges (Fig. 1). Unit  $\text{CaWO}_4$  cell is tetragonal with cell parameters  $a = b = 5.24318 \text{ \AA}$  and  $c = 11.37104 \text{ \AA}$  according to Inorganic Crystal Structure Database (ICSD) card N° 15586. X-Fit [30] was used to extract the unit cell parameters through peak fitting analysis, which determines the unit cell parameter from least squares analysis of the positions of the peaks. The value crystallite size was 177 nm. In principle, this is expected, because the test sample obtained by milling of the single crystals. The crystallites were significantly larger and out of range of accurate measurement using XRD methods. On the other hand, the size of microstrain (0.276 %) is high, which is also characteristic of the samples obtained by milling of the single crystal.

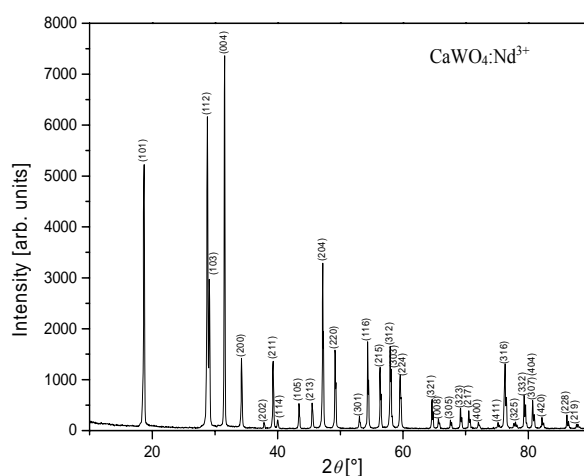


**Fig. 5.** XRD pattern of  $\text{CaWO}_4:\text{Nd}^{3+}$ . All peaks are indexed according to 88. space group,  $I4_1/a$ .

Factor group analysis in the C space group gives the following set of irreducible representations that characterize all the vibration modes (Raman and infrared) for a tetragonal scheelite primitive cell ( $k=0$ ) [35, 36]:

$$\Gamma_{(\text{Raman} + \text{Infrared})} = 3A_g + 5B_g + 5E_g + 5A_u + 3B_u + 5E_u \quad (1)$$

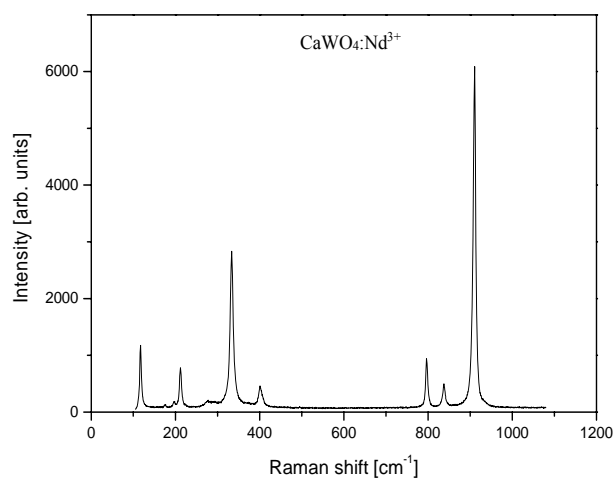
where the  $A_g$ ,  $B_g$  and  $E_g$  are Raman-active modes. The A and B modes are nondegenerate, while the E modes are doubly degenerate. The subscripts 'g and u' indicate the parity under inversion in centrosymmetric  $\text{CaWO}_4$  crystals. The  $A_u$  and  $E_u$  modes correspond to the zero frequency of acoustic modes, while the others are optic modes. In addition, the  $A_g$ ,  $B_g$  and  $E_g$  modes arise from the same motion in a  $\text{CaWO}_4$  phase. Thus, 13 zone-center Raman-active modes for the  $\text{CaWO}_4$  crystals are expected, as described in Eqn. (2) [37, 38]:

$$\Gamma_{(\text{Raman})} = 3A_g + 5B_g + 5E_g \quad (2)$$

According to the literature [39, 40], the vibrational modes detected in the Raman spectra of tungstates can be classified into two groups, external and internal modes [41]. In vibrational infrared spectra,  $1A_u$  and  $1E_u$  acoustic are infrared-inactive mode and  $3B_u$  forbidden infrared modes. Therefore, only 8 infrared-active vibration modes remain, as presented by Eqn. (3) [42]:

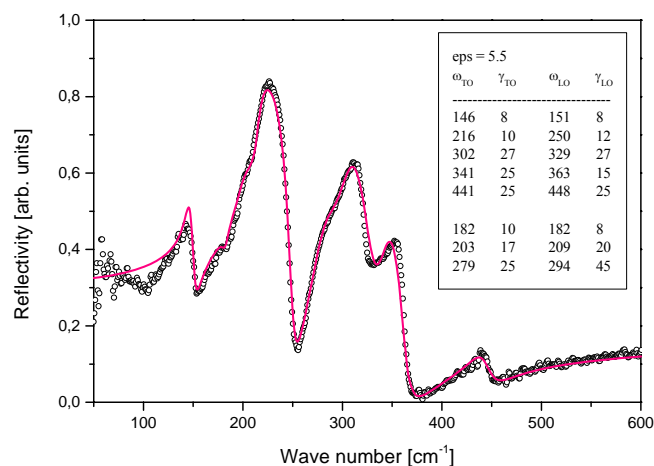
$$\Gamma_{(\text{Infrared})} = 4A_u + 4E_u \quad (3)$$

Fig. 6 shows a Raman spectrum of the  $\text{CaWO}_4:\text{Nd}^{3+}$  excited 532 nm line of an Ar-ion laser kept at a power of 0.25 mW on sample. The internal vibrations are related to the  $[\text{WO}_4]^{2-}$  molecular group with a stationary mass center. The external vibrations or lattice phonons are associated to the motion of the  $\text{Ca}^{2+}$  cation and rigid molecular units. In the free space,  $[\text{WO}_4]^{2-}$  tetrahedrons show  $T_d$ -symmetry. In this case, the vibrations of the  $[\text{WO}_4]^{2-}$  ions are constituted by four internal modes ( $\nu_1(A_1)$ ,  $\nu_2(E)$ ,  $\nu_3(F_2)$  and  $\nu_4(F_2)$ ), one free rotation mode ( $\nu_{\text{fr}}(F_1)$ ) and one transition mode ( $F_2$ ). When  $[\text{WO}_4]^{2-}$  ions are present in a scheelite-type structure, its point symmetry reduces to  $S_4$ . The  $3B_u$  vibration is a silent mode. The Raman modes in Fig. 6 were detected as  $\nu_1(A_g)$ ,  $\nu_3(B_g)$ ,  $\nu_3(E_g)$ ,  $\nu_4(B_g)$ ,  $\nu_2(B_g)$ , rotation ( $E_g$ ) and rotation ( $A_g$ ) vibrations at 912, 835, 798, 395, 329, 281 and 216  $\text{cm}^{-1}$ , respectively, which provide evidence of a Scheelite structure. The well-resolved sharp peaks for the  $\text{CaWO}_4$  indicate that the synthesized particles are highly crystallized.



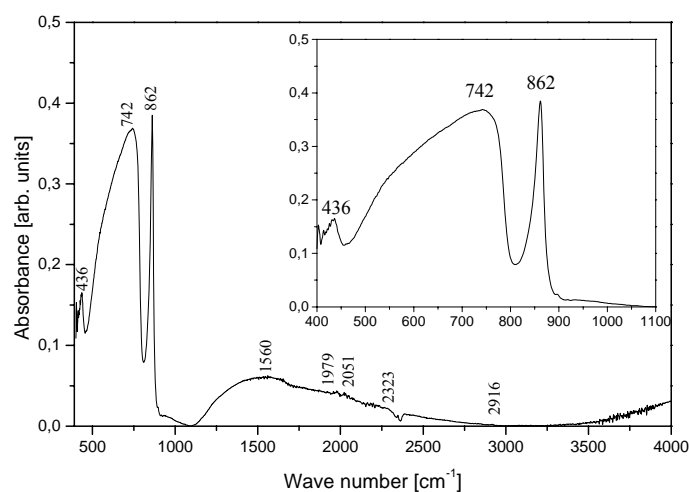
**Fig. 6.** Raman spectrum of  $\text{CaWO}_4:\text{Nd}^{3+}$  single crystal, recorded at room temperature.

Fig. 7 illustrate the IR spectrum and corresponding positions of IR-active modes of crystal. The tungstates with scheelite-type structure have eight stretching and/or bending IR-active vibrational modes [43, 44]. In our case, no more than six modes [ $2A_u$ ,  $1(A_u + E_u)$  and  $3E_u$ ] were identified in the spectra (Fig. 7).



**Fig. 7.** IR spectrum of  $\text{CaWO}_4:\text{Nd}^{3+}$  single crystal, recorded at room temperature.

Fig. 8 shows FTIR spectrum of the obtained  $\text{CaWO}_4:\text{Nd}^{3+}$  at the wavenumber range of  $4000\text{--}400\text{ cm}^{-1}$ . The band at around  $2916\text{ cm}^{-1}$  correspond to the stretching vibration of the hydroxyl ion [45]. The band at  $2323\text{ cm}^{-1}$  shows the existence of  $\text{CO}_2$ . The bands below  $1000\text{ cm}^{-1}$  are characteristic of the W-O bond. The absorption band at around  $742\text{ cm}^{-1}$  and strong band at  $862\text{ cm}^{-1}$  are attributed to the O-W-O stretches of the  $[\text{WO}_4]^{2-}$  tetrahedron, because the  $\text{AWO}_4$ -type scheelite oxides  $S_4$  site symmetry for the  $\text{WO}_4$  groups [45, 46]. The weak vibration band detected at  $436\text{ cm}^{-1}$  could be ascribed to the W-O bending vibration [47]. The band at  $1560\text{ cm}^{-1}$  corresponds to the O-H stretching and the H-O-H bending vibrations, due to small quantity of surface-absorbed water [47, 48]. From the FTIR spectrum (Fig. 7), a strong peak at  $862\text{ cm}^{-1}$  has been obtained due to the stretching vibration of  $[\text{WO}_4]^{2-}$  in scheelite structure, and a weak but sharp band at  $433\text{ cm}^{-1}$  has also been noticed due to the metal, oxygen (Ca-O) band.



**Fig. 8.** FTIR spectrum of  $\text{CaWO}_4:\text{Nd}^{3+}$  single crystal.



Near infrared luminescence of  $\text{Nd}^{3+}$  doped phosphors have received the renewed interest recently [49-51]. The time resolved optical characteristics of samples were analyzed using streak camera and Nd:YAG laser as excitation source. The setup is described in more detail in our earlier publication [34]. Here, we use pulsed laser excitation at 532 nm for time resolved analysis of  $\text{CaWO}_4:\text{Nd}^{3+}$  near infrared luminescence. We have analyzed the part of the spectrum corresponding to  ${}^4\text{F}_{5/2} - {}^4\text{I}_{9/2}$  and  ${}^4\text{F}_{3/2} - {}^4\text{I}_{9/2}$  transitions. These transitions are of interest for remote temperature sensing, as described in [49-51]. Fluorescence intensity ratio of these two transitions is used to determine temperature sensing calibration curves. The analyzed samples of  $\text{SrF}_2:\text{Nd}^{3+}$  [49], and  $\text{La}_2\text{O}_3:\text{Nd}^{3+}$  [50] phosphors were excited by CW laser at 532 nm. The extensive study of using  $\text{Nd}^{3+}$ -based luminescent nanothermometers is provided in [51]. Streak images of near infrared luminescence of  $\text{Nd}^{3+}$  doped crystal is shown in Fig. 9.

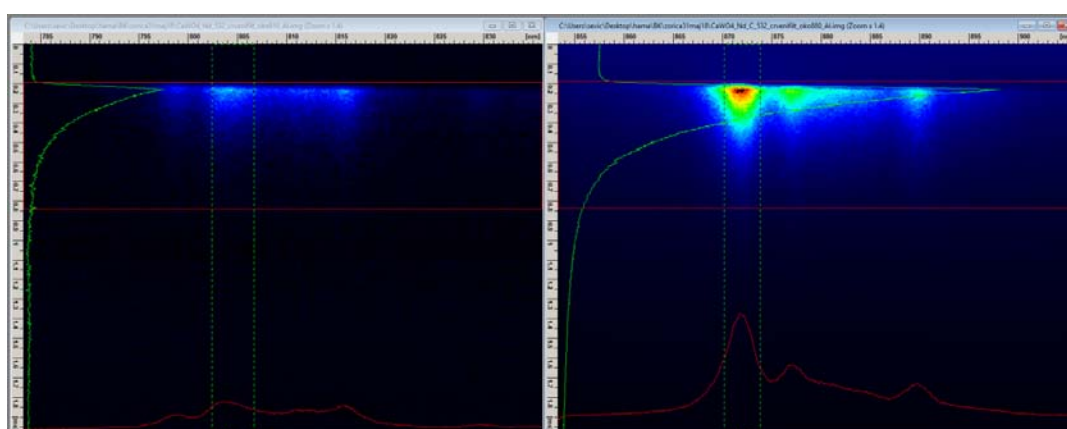


**Fig. 9.** Streak images of  $\text{CaWO}_4:\text{Nd}^{3+}$  luminescence emission, excited at 532 nm. Bands around 810 nm ( ${}^4\text{F}_{5/2} - {}^4\text{I}_{9/2}$  transition) and around 880 nm ( ${}^4\text{F}_{3/2} - {}^4\text{I}_{9/2}$  transition) were recorded separately, using diffraction grating of  $300 \text{ g mm}^{-1}$  for better wavelength resolution.

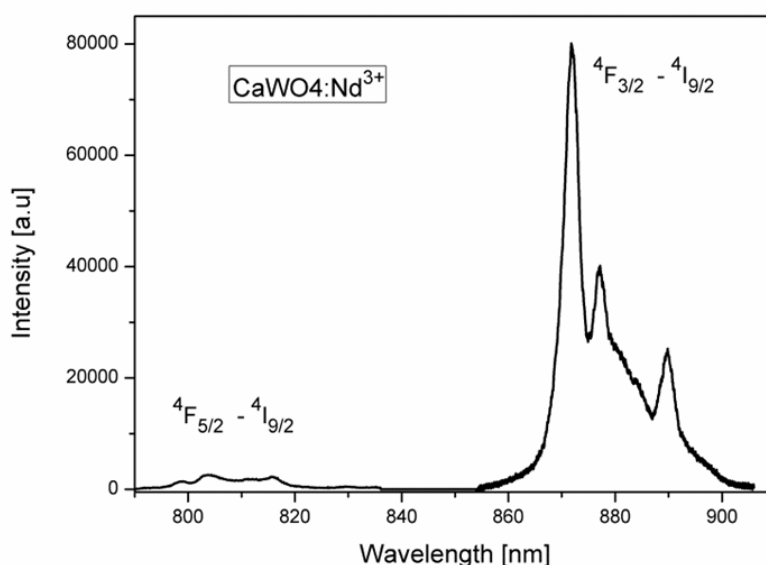


**Fig. 10.** Near infrared spectrum of  $\text{CaWO}_4:\text{Nd}^{3+}$  luminescence excited at 532 nm.

We have used HPD-TA software, provided by Hamamatsu, to calculate the lifetime of  $\text{CaWO}_4:\text{Nd}^{3+}$  luminescence. Estimated luminescence lifetime of  ${}^4\text{F}_{5/2} - {}^4\text{I}_{9/2}$  transition is



about 120  $\mu\text{s}$ ; estimated luminescence lifetime of  ${}^4\text{F}_{3/2} - {}^4\text{I}_{9/2}$  transition is about 140  $\mu\text{s}$ . This result (regarding the  ${}^4\text{F}_{3/2} - {}^4\text{I}_{9/2}$  transition) is almost the same as provided in [51], ( $\text{Gd}_2\text{O}_3:\text{Nd}^{3+}$ ), where corresponding lifetime at room temperature is about 142  $\mu\text{s}$ . Our results are not far from the value of 220  $\mu\text{s}$  provided in table 4 of [52], where  $\text{Nd}^{3+}$  doped BGO crystal was analyzed. Comparing our results with a few results provided in other references, we see that the lifetimes could be strongly dependent on host [53]. Measured lifetimes for the same transitions in [49], ( $\text{SrF}_2:\text{Nd}^{3+}$ ) are about 5  $\mu\text{s}$  for  ${}^4\text{F}_{5/2} - {}^4\text{I}_{9/2}$  transition and about 1230  $\mu\text{s}$  for  ${}^4\text{F}_{3/2} - {}^4\text{I}_{9/2}$  transition. Fig. 10 shows near infrared spectrum of  $\text{CaWO}_4:\text{Nd}^{3+}$  luminescence excited at 532 nm, obtained by background and sensitivity correction of streak images presented in Fig. 9.

The properties of the crystal, such as density of dislocations, crystallinity, and impurities concentrations, determine the optical quality.

#### 4. Conclusion

$\text{Nd}^{3+}$  doped calcium tungstate single crystals were grown from melt using the Czochralski method in air. The value of the crystal growth rate was experimentally found to be 6.7 mm  $\text{h}^{-1}$ . The critical diameter of obtained crystal was about 10 mm. The obtained transparent light blue single crystal and powdered sample were characterized by X-ray diffraction, Raman and IR spectroscopy. The XRD confirms that sample is monophase, and that it crystallized in scheelite type of structure in 88. space group,  $I4_1/a$ . A good correlation was found between the experimental and theoretical Raman and infrared active modes. FTIR confirmed the occurrence of all the functional groups and bonds in this material. From the FTIR spectrum, a strong peak of 862  $\text{cm}^{-1}$  has been obtained due to the stretching vibration of  $\text{WO}_4^{2-}$  in scheelite structure, and a weak but sharp band at 433  $\text{cm}^{-1}$  has been noticed due to the metal, oxygen (Ca-O) band. Micro hardness was measured with the Vickers pyramid. Anisotropy in [001] direction was not observed. The crystal showed a micro hardness of 1.5 GPa. Based on our work and observations during the experiment, it could be concluded that the obtained  $\text{CaWO}_4:\text{Nd}^{3+}$  single crystal is of good optical quality, which was the goal of our work.

#### Acknowledgments

This research was financially supported by the Ministry of Education, Science and Technological Development of the Republic of Serbia through Projects No. III 45003 and TR34011.

#### 5. References

1. G. Jia, C. Wang, S. Xu, J. Phys. Chem. C, 114 (2010) 17905.
2. X. Yan-Ling, Z. Hong, W. Rui, Z. Chun-Yu, Chin. Phys. Lett., 6 (2011) 064210.
3. H. Lei, S. Zhang, XZ. Zhu, Y. Sun, Y. Fu, Mater.Lett., 64 (2010) 344.
4. D. Errandonea, R. S. Kumar, X. Ma, C. Tu, J. Solid State Chem., 181 (2008) 355.
5. V. I. Balakshy, K. Asratyan, V. Y. Molchanov, J. Opt. A: Pure Appl. Opt., 3 (2001) S87.
6. L. Fan, Y. X./ Fan, Y. H. Duan, Q. Wang, H. T. Wang, G. H. Jia, C. Y. Tu, Appl. Phys. B: Lasers Opt., 94 (2009) 553.
7. J. Sulc, H. Jelinkova, T. T. Basiev, M. E. Doroschenko, L. I. Ivleva, V. V. Osiko, P. G. Yverev, Opt. Mater., 30 (2007) 195.

8. P. G. Yang, J. Liu, H. Yang, X. Yu, Y. Guo, Y. Zhou, J. Liu, *J. Mater. Chem.*, 19 (2009) 3771.
9. J. Bi, L. Wu, Y. Zhang, Z. Li, j. Li, X. Fu, *Appl. Catal. B*, 91 (2009) 135.
10. J. Yu, L. Qi, B. Cheng, X. Zhao, *J. Hazard. Mater.*, 160 (2008) 621.
11. J. Liu, H. Lian, C. shi, *Opt. Mater.*, 29 (2007) 1591.
12. J. Liao, B. Qiu, H. Wen, J. Chen, W. You, *Mater. Res. Bull.*, 44 (2009) 1863.
13. J. Liao, B. Qiu, H. Wen, J. Chen, W. You, L. Liu, *J. Alloys Compd.*, 487 (2009) 758.
14. A. V. Vereswnikova, B. K. Lubsandorzhev, I. R. Barabanov, P. Grabmayr, D. Greiner, J. Jochum, M. Knapp, C. Ostwald, R. V. Poleshuk, F. Ritter, B. A. M. Shaibonov, Y. E. Vyatchin, G. Meierhofer, *Nucl. Instrum. Methods Phys. Res. Sect. A*, 603 (2009) 529.
15. V. B. Mikhailika, S. Henrya, H. Krausa, I. Solskii, *Nucl. Instrum. Methods Phys. Res. Sect. A*, 583 (2007) 350.
16. I. Annenkov, O. A. Buzanov, F. A. Danevich, A. Sh. Georgadze, S. K. Kim, H. J. Kim, Y. D. Kim, V. V. Kobychhev, V. N. Kornoukhov, M. Korzhik, J. I. Lee, O. Missevitch, V. M. Mokina, S. S. Nagorny, A. S. Nikolaiko, D. V. Poda, R. B. Podvianuk, D. J. Sedlak, O. G. Shkulkova, J. H. So, I. M. Solsky, V. I. Tretyak, S. S. Yurchenko, *Nucl. Instrum. Methods Phys. Res. Sect. A*, 584 (2008) 334.
17. G. K. Choi, J. R. Kim, S. H. Yoon, K. S. Hong, *J. Eur. Ceram. Soc.*, 27 (2007) 3063.
18. G. K. Choi, S. Y. Cho, J. S. An, K. S. Hong, *J. Eur. Ceram. Soc.*, 26 (2006) 2011.
19. H. Kraus, V. B. Mikhailik, *Nucl. Instrum. Methods Phys. Res. Sect. A*, 621 (2010) 395.
20. J. Ninkovic, G. Angloher, C. Bucci, C. Cozzini, T. Frank, D. Hauff, H. Kraus, B. Majorovits, V. Mikhailik, F. Petricca, F. Probat, Y. Ramachers, W. Rau, W. Seidel, S. Uchaikin, *Nucl. Instrum. Methods Phys. Res. Sect. A*, 537 (2005) 339.
21. I. Trabelsi, M. Dammak, R. Maalej, M. Kamoun, *Phys. B*, 406 (2011) 315.
22. W. Wang, P. Yang, S. Gai, N. Niu, F. He, J. Lin, *J. Nanopart. Res.*, 12 (2010) 2295.
23. Q. Xiao, Q. Zhou, M. Li, *J. Lumin.*, 130 (2010) 1092.
24. A. B. Campos, A. Z. Simões, E. Longo, J. A. Varela, V. M. Longo, A. T. de Figueiredo, F. S. de Vicente, A. C. Hernandez, *Appl. Phys. Lett.*, 91 (2007) 051923.
25. L. S. Cavalcante, V. M. Longo, J. C. Sczancoski, M. A. P. Almeida, A. A. Batista, J. Varela, M. O. Orlandi, E. Longo, M. Siu Li, *Cryst. Eng. Comm.*, 14 (2012) 853.
26. I. V. Andreiev, V. p. Bondarenko, L. G. Tarasenko, *Sci. Sinter.*, 48 (2016) 191.
27. C. Tablero, *Chem. Phys. Lett.*, 635 (2015) 190.
28. R. M. Hazen, L. W. Finger, J. W. E. Mariathan, *J. Phy. Chem. Solids*, 46 (1985) 253.
29. A. Golubovic, R. Gajic, Z. Dohcevic, S. Nikolic, *Sci. Sinter.*, 38 (2006) 265.
30. R. W. Cheary, A. Coelho, *J. Appl. Crystallography*, 25 (1992) 109.
31. H. I. Elswie, Z. Ž. Lazarević, V. Radojević, M. Gilić, M. Rabasović, D. Šević, N. Ž. Romčević, *Sci. Sinter.*, 48 (2016) 333.
32. M. A. Almessiere, *Sci. Sinter.*, 50 (2018) 63.
33. M. Petrović, M. Gilić, J. Ćirković, M. Romčević, N. Romčević, J. Trajić, I. Yahia, *Sci. Sinter.*, 49 (2017) 167.
34. M. S. Rabasovic, D. Sevic, M. Terzic, B. P. Marinkovic, *Nucl. Inst. Meth.*, B 279 (2012) 16.
35. M. Crane, R. L. Frost, P. A. Williams, J. T. Klopogge, *J. Raman Spectrosc.*, 33 (2002) 62.
36. R. L. Rousseau, R. P. Bauman, S. P. Porto, *J. Raman Spectrosc.*, 10 (1981) 253.
37. D. Christofilos, G. A. Kourouklis, S. Ves, *J. Phys. Chem. Solids*, 56 (1995) 1125.
38. S. P. S. Porto, J. F. Scott, *Phys. Rev.*, 157 (1967) 716.
39. M. Nicol, J. F. Durana, *J. Chem. Phys.*, 54 (1971) 1436.
40. T. T. Basiev, A. A. Sobol, Y. K. Voronko, P. G. Zverev, *Opt. Mater.*, 15 (2000) 205.

41. A. Phuruangrat, T. Thongtem, S. Thongtem, J. Exp. Nanosci., 5 (2010) 263.
42. T. T. Basiev, A. A. Sobol, P. G. Zverev, I. I. Ivleva, V. V. Osiko, R. C. Powell, Opt. Mater., 11 (1999) 307.
43. A. S. Barker Jr., Phys. Rev., 135 (1964) A742.
44. Z. C. Ling, H. R. Xia, D. G. Ran, F. Q. Liu, S. Q. Sun, J. D. Fan, H. J. Zhang, J. Y. Wang, L. L. Yu, Chem. Phys. Lett., 426 (2006) 85.
45. P. Suneetha, Ch. Rajesh, M. V. Ramana, Mater. Res. Express, 4 (2017) 085020.
46. Q. Li, Y. Shen, T. Li, J. Chem., 2013 (2013) 952954.
47. N. A. Sabu, X. Francis, J. Anjaly, S. Sankararaman, T. Varghese, Eur. Phys. J. Plus, 32 (2017) 290.
48. X. Lai, Y. Wei, D. Qin, Y. Zhao, Y. Wu, D. Gao, J. Bi, D. Lin, G. Xu, Integr. Ferroelec., 142 (2013) 7.
49. N. Rakov, G. S. Maciel, J. Appl. Phys., 121 (2017) 113103.
50. G. Jiang, X. Wei, S. Zhou, Y. Chen, C. Duan, M. Yin, J. Lumin., 152 (2014) 156.
51. S. Balabhadra, M. L. Debasu, C. D. S. Brites, L. A. O. Nunes, O. L. Malta, J. Rocha, M. Bettinellie, L. D. Carlos, Nanoscale, DOI: 10.1039/c5nr05631d.
52. F. Chen, M. Ju, G. L. Gutsev, X. Kuang, C. Lu, Y. Yeung, J. Mater. Chem. C, 5 (2017) 3079.
53. X. Fu, Z. Jia, Y. Li, D. Yuan, C. Dong, X. Tao, Opti. Mat. Express, 2 (2012) 1242.

**Садржај:** Циљ овог рада је био да се добије монокристал калцијум волфрамата допиран са неодимијумом - ( $\text{CaWO}_4:\text{Nd}^{3+}$ ), а након тога добијени кристал карактерише са различитим спектроскопским методама. Монокристал је добијен методом раста кристала по Чокралском на ваздуху. Оптимизацијом услова раста, добијени су  $\text{CaWO}_4:\text{Nd}^{3+}$  кристали  $\langle 001 \rangle$ -оријентације пречника до 10 милиметара. Број дислокација у добијеном кристалу је 102 по центиметру квадратном. Микро тврдоћа је мерена са Вицкерс пирамидом. Анизотропија у  $\langle 001 \rangle$  правцу није примећена. Одабрани  $\text{CaWO}_4:\text{Nd}^{3+}$  кристал је сечен на неколико плочица дијамантском тестером. Плочице су полиране дијамантском пастом. Кристална структура је потврђена рендгенском дифракционом анализом. Добијени кристал је испитиван методам Раман и инфрацрвеном спектроскопијом. У складу са теоријом група примећено је седам Раман и шест инфрацрвених оптичких модова. Фуријеовом трансформационом инфрацрвеном спектроскопијом је потврђена појава свих карактеристичних функционалних група и веза у овом материјалу. Из ФТИР спектра, добијен је изражен пик на  $862 \text{ cm}^{-1}$  услед вибрације истежања  $\text{WO}_4^{2-}$  у шелитној структури, а слаб али оштар пик на  $433 \text{ cm}^{-1}$  је примећен због везе метал-кисеоник (Ca-O). Процењено време живота луминисценције  $^4\text{F}_{5/2} - ^4\text{I}_{9/2}$  је око  $120 \mu\text{s}$ ; процењено време живота луминисценције  $^4\text{F}_{3/2} - ^4\text{I}_{9/2}$  је око  $140 \mu\text{s}$ . Сва обављена истраживања показују да добијени монокристал  $\text{CaWO}_4:\text{Nd}^{3+}$  има добар оптички квалитет, што је и био циљ овог рада.

**Кључне речи:**  $\text{CaWO}_4:\text{Nd}^{3+}$ , Раман спектроскопија, инфрацрвена спектроскопија, луминисценција.

